Atmos. Chem. Phys. Discuss., 13, 23023–23056, 2013
www.atmos-chem-phys-discuss.net/13/23023/2013/
doi:10.5194/acpd-13-23023-2013

Atmospheric Chemistry and Physics Discussions

Estimation of cloud condensation nuclei concentration from aerosol optical quantities: influential factors and uncertainties

J. Liu and Z. Li

Department of Atmospheric and Oceanic Science and Earth System Science Interdisciplinary Center, University of Maryland, College Park, Maryland, USA

Received: 26 July 2013 – Accepted: 19 August 2013 – Published: 2 September 2013

Correspondence to: Z. Li (zli@atmos.umd.edu)

Published by Copernicus Publications on behalf of the European Geosciences Union.

Abstract

Cloud condensation nuclei (CCN) is a key variable for understanding cloud formation, but it is hard to obtain on large scales on a routine basis, whereas aerosol optical quantities are more readily available. This study presents an in-depth investigation on the relationship between CCN and aerosol optical quantities in regions of distinct aerosol types using extensive measurements collected at multiple Atmospheric Radiation Measurement (ARM) Climate Research Facility (CRF) sites around the world. The influences of relative humidity (RH), aerosol hygroscopicity (f_{RH}) and single scattering albedo (SSA) on the relationship are analyzed. Better relationships are found between aerosol optical depth (AOD) and CCN at the Southern Great Plains (US), Ganges Valley (India) and Black Forest sites (Germany) than those at the Graciosa Island and Niamey (Niger) sites, where sea salt and dust aerosols dominate, respectively. In general, the correlation between AOD and CCN decreases as the wavelength of AOD measurement increases, suggesting that AOD measured at a shorter wavelength is a better proxy of CCN. The correlation is significantly improved if aerosol index (AI) is used together with AOD. The highest correlation exists between CCN and aerosol scattering coefficients (σ_{sp}) and scattering AI measured in-situ. The CCN-AOD (AI) relationship deteriorates with increasing RH. If RH exceeds 75 %, the relationship becomes almost invalid for using AOD as a CCN proxy, whereas a tight σ_{sp}-CCN relationship exists for dry particles. Aerosol hygroscopicity has a weak impact on the σ_{sp}-CCN relationship. Particles with low SSA are generally associated with higher CCN concentrations, suggesting that SSA affects the relationship between CCN concentration and aerosol optical quantities. It may thus be used as a constraint to reduce uncertainties in the relationship. A significant increase in σ_{sp} and decrease in CCN with increasing SSA is observed, leading to a significant decrease in their ratio (CCN/σ_{sp}) with increasing SSA. The relationships and major influential factors are parameterization for improving CCN estimation with varying amount of information on RH, particle size and SSA.

ACPD
13, 23023–23056, 2013

1 Introduction

It has been well recognized that aerosols play important roles in Earth's climate and the hydrological cycle via their direct and indirect effects (IPCC, 2007). Aerosol particles can scatter and absorb solar radiation, alter the vertical distribution of solar energy and atmospheric stability (Ramanathan et al., 2001; Liu et al., 2012). These are known as direct effects. Aerosols can modify microphysical and macroscopic cloud properties, such as cloud particle size, cloud albedo (Twomey, 1977; Twomey et al., 1984; Rosenfeld et al., 2001; Andreae et al., 2004; Koren et al., 2005) and cloud-top heights (Andreae et al., 2004; Lin et al., 2006; Li et al., 2011). They can also influence warm- and cold-rain processes (Rosenfeld and Woodley, 2000; Andreae et al., 2004; Lin et al., 2006; Bell et al., 2008; Li et al., 2011), the depth of the mixed-phase region in a cloud (Andreae et al., 2004; Koren et al., 2005, 2008, 2010; Niu and Li, 2011) and the occurrence of lightning (Orville et al., 2001; Steiger and Orville, 2003; Yuan et al., 2011; Yang et al., 2013). These are known as indirect effects. One of the greatest sources of uncertainty in climate modeling is the treatment of indirect effects of aerosols on cloud optical depth through the role of aerosols as cloud condensation nuclei (CCN) (Ghan et al., 2006). Determining CCN concentrations and their spatial and temporal variations are key challenges in quantifying aerosol indirect effects.

CCN concentration has been measured chiefly through field experiments by counting the number of droplets formed in a chamber using optical counters at various levels of water vapor supersaturation (Hudson and Yum, 2002; Ross et al., 2003; Yum et al., 2007; Rose et al., 2008; J. Liu et al., 2011). However, such in-situ measurements of CCN concentration are few and localized and thus may not represent large areas. Extensive measurements of CCN concentration are not currently feasible because of the high cost and complex nature of the operation. CCN is determined by the aerosol size distribution and chemical composition governed by the Köhler theory. Aerosol particles in the ambient environment are often very complex and are comprised of inorganic and organic species (Kanakidou et al., 2005; Zhang et al., 2007), so the Köhler theory has

ACPD
13, 23023–23056, 2013

been extended to include the influence of these species (Shulman et al., 1996; Facchini et al., 1999; Svenningsson et al., 2005). The mixing state and a detailed knowledge of how different compounds interact with water also matter (McFiggans et al., 2006; Andreae and Rosenfeld, 2008; Ward et al., 2010; Yang et al., 2011). A modified Köhler theory, called the "κ-Köhler" theory, was proposed by Petter and Kriedenweis (2007), which uses a single parameter, κ, to describe the solubility effect on CCN activation.

Unlike CCN concentration and size-resolved aerosol composition, aerosol optical quantities such as aerosol optical depth (AOD) and aerosol scattering/extinction coefficients, are much more readily available from ground-based and space-borne remote sensing instruments. Thus aerosol optical quantities, especially AOD, have often been used as a proxy for CCN in large-scale model simulations (Quaas et al., 2009; Wang et al., 2011; Tao et al., 2012; Grandey et al., 2013) and in studying aerosol indirect effects (Nakajima, 2001; Bréon et al., 2002; Feingold, 2003; Yuan, 2008). However, AOD represents the vertically integrated attenuation and depends not only on the number of particles but also on relative humidity (RH), size distribution, etc, and might not be a good proxy for CCN (Jeong et al., 2007). The use of aerosol optical measurements to estimate CCN concentrations is appealing but challenging because they are governed by different aerosol attributes (Ghan et al., 2006; Kapustin et al., 2006; Andreae, 2009). Nevertheless, attempts at relating CCN concentration to AOD or aerosol extinction/scattering properties showed gross correlations between CCN concentration and aerosol optical quantities (Ghan and Collins, 2004; Ghan et al., 2006; Shinozuka et al., 2009; Andreae, 2009; Jefferson, 2010; J. Liu et al., 2011). The correlation is often fraught with uncertainties that could be reduced by accounting for some influential factors such as aerosol size and/or composition, as well as environmental variables (e.g., RH), but few systematic investigations were conducted (Andreae, 2009), due partially to few extensive measurements being available.

Thanks to the US Department of Energy for deploying the Atmospheric Radiation Measurement (ARM) Climate Research Facility (both at fixed and mobile locations), CCN and many pertinent variables have been made in recent years, allowing for the

ACPD
13, 23023–23056, 2013

study as presented here. The goal is to gain further insights into the relationship between CCN and aerosol optical quantities such as columnar AOD and aerosol scattering coefficients by exploiting rich ARM data acquired around the world with different background aerosol types. Influences on the relationship is investigated of RH, aerosol hygroscopicity and aerosol single scattering albedo (SSA) for reducing the uncertainty in estimating CCN from aerosol optical measurements. Measurements and methods used are described in Sect. 2. Section 3 presents results from various analyses and a summary is given in Sect. 4.

2 Data and methodology

2.1 Data

ARM data are at five sites are employed here, representing different regions (e.g., continental and marine) dominated by different types of aerosols: the US Southern Great Plains (SGP, permanent site, typical rural continental aerosols over farm land), Graciosa Island in the Azores (GRW, mobile facility site, sea salt aerosols and local pollution from airport traffic and long-range transport from Europe), the Black Forest in Germany (FKB, mobile facility, agricultural and forested regions with rich biogenic aerosols), the Ganges Valley in India (GVAX, mobile facility: anthropogenic pollution, high concentrations of sulfate, nitrate, organic and black carbon contents), and Niamey in Niger (NIM, mobile facility, dust aerosols). The locations and observation periods, as well as measurements used in this study, are listed in Table 1. More detailed information about each site can be found at http://www.arm.gov/sites.

AOD and the Angstrom wavelength exponent (α) were from the NASA Aerosol Robotic Network (AERONET) database, which are available at http://aeronet.gsfc.nasa.gov (Holben et al., 1998). There were no AERONET retrievals available for the FKB site. Cimel sunphotometers used in the AERONET measure direct solar and sky radiances at discrete wavelengths (340, 380, 440, 500, 670, 870, 940 and 1020 nm)

ACPD
13, 23023–23056, 2013

from which AOD is retrieved at each wavelength with uncertainty of 0.01–0.02 (Dubovik and King, 2000). At the FKB site, AOD and α were retrieved from the Multifilter rotating shadowband radiometer (MFRSR). It measures total and diffuse solar broadband irradiances at 415, 500, 610, 673, 870, and 940 nm with AOD retrieval accuracy of ~ 0.01 (Alexander et al., 2008).

CCN and aerosol condensation nuclei (CN) concentrations, aerosol scattering and absorption properties, as well as the aerosol hygroscopic growth factor (f_{RH}), were measured by a suite of instruments comprising the aerosol observing system (AOS), which is the primary ARM platform measuring in situ aerosol properties at the surface (Jefferson, 2005). CN concentrations were measured by the TSI Model 3010 instrument, which is a compact and rugged instrument that counts the number of particles with particle diameters in the size range of 10 nm to 3 µm. CCN concentrations were measured by the Droplet Measurement Technology (DMT) continuous flow CCN counter at seven levels of super-saturation (Roberts and Nenes, 2005). The observation interval is 5 min at each level of super-saturation. It is calibrated at the beginning and the end of each mobile facility deployment and annually at the SGP site (Jefferson, 2005).

The integrated aerosol scattering coefficients (σ_{sp}) over the scattering angle range (7–170°) were measured with TSI Model 3565 three-wavelength (450, 550 and 700 nm) nephelometers that separate aerosols by particle diameter for total aerosols ($D_p \leq$ 10 µm) and submicrometer aerosols ($D_p \leq 1$ µm). Two nephelometers were deployed with one serving as the "reference" that measures dry aerosol scattering coefficients and the other is connected to a humidity scanning system in order to measure changes in aerosol scattering coefficient with RH. The humidifier scans RH from low (~ 40 %) to high (~ 90 %) and back to low RH on an hourly basis. Aerosol light absorption coefficients (σ_{ap}) at 470, 528 and 660 nm were measured by a filter-based Radiances Research particle/soot absorption photometer (PSAP). The 470 nm absorption coefficient was normalized to 450 nm in order to match with the scattering coefficient measured by the nephelometer. The uncertainty in σ_{sp} measured by the nephelometer was inves-

ACPD
13, 23023–23056, 2013

tigated by Anderson et al. (1996) and Heintzenberg et al. (2006), usually ranging from 1 to 4 Mm^{-1} for one-minute averaged data. It also depends on the magnitudes of the absorption and scattering coefficients (Jefferson et al., 2005).

Aerosol hygroscopic growth factor, f_{RH} is a common way to quantify a measure of the increase in aerosol scattering relative to a dry scattering with changes in relative humidity, and is defined as the ratio of the σ_{sp} at a given RH to that at a low reference RH:

$$f_{RH(RH/RH_{Ref})} = \sigma_{sp(RH)}/\sigma_{sp(RH_{Ref})} \quad (1)$$

This hygroscopic growth factor at RH = 85 % and RH_{Ref} = 40 % is then expressed as $f_{RH(85\,\%/40\,\%)}$. To calculate the RH dependence of aerosol scattering coefficients, a two-parameter empirical fits are used here (Jefferson et al., 2005):

$$f_{RH} = a \times \left(1 - \frac{RH(\%)}{100}\right)^{-b} \quad (2)$$

where a and b are determined from σ_{sp} at low (~ 40 %) and high RH levels (e.g. Jeong et al., 2007). Knowing the fit parameters, one can estimate σ_{sp} at any ambient RH:

$$\sigma_{sp}(amb) = \sigma_{sp}(dry)\frac{(1 - RH_{amb}/100)^{-b}}{(1 - RH_{dry}/100)^{-b}} \quad (3)$$

2.2 Data analysis

After matching data from multiple instruments according to observation time, they are sorted into different discrete bins in which means and standard deviations are calculated. To be consistent with Andreae (2009), we also use CCN concentration at S = 0.4 % in this study. To increase sample size, CCN measured at any level of supersaturation is adjusted to a fixed supersaturation of 0.4 % following:

$$CCN_S = N_0(1 - \exp(-bS^k)) \quad (4)$$

ACPD
13, 23023–23056, 2013

where CCN_S is the number concentration of CCN at the supersaturation S, N_0, b and k are empirical fitted parameters (Ji and Shaw, 1998). This function describes the $N_{CCN} \sim S$ relationship is better than $CCN_S = CS^k$ suggested by Twomey (1959) (C and k are fitted parameters) since the Twomey formula overestimates CCN concentration at large S and predicts unconstrained CCN with increasing total aerosol concentration. The mean error of the fitted CCN concentration in our study is about 9.5 %, 3.2 %, 6.3 %, 23.8 % and −10.7 % at SGP, GRW, NIM, GVAX and FKB site, respectively.

3 Results

3.1 Overall correlation between aerosol optical quantities and CCN

Table 2 presents the means and standard deviations of aerosol optical quantities and CCN at all the sites. The largest mean AOD occurred at the NIM site (0.39 ± 0.33), almost four times greater than that at other sites, and the smallest mean AOD at the GRW site (0.11 ± 0.06). Mean α at these two locations (NIM: 0.47 ± 0.23, GRW: 0.75 ± 0.35) are lower than at the other sites, indicating more influence of coarse particles (dust particles at the NIM site and sea salt at the GRW site). The largest mean α at the FKB site (1.88 ± 0.27) suggests more fine particles at this site than at the SGP and GVAX sites. Mean σ_{sp} show that submicron particles ($D_p \leq 1$ µm) play a dominant role in aerosol scattering at the SGP and FKB sites. They are responsible for nearly half of the aerosol scattering at the NIM and GVAX sites. Coarse particles with diameters > 1 µm contribute more to aerosol scattering at the GRW site. The smallest values of single scattering albedo (SSA) are found at the NIM and FKB sites (0.82 ± 0.06 and 0.85 ± 0.06, respectively). As per the values of SSA and α, significantly different aerosol types are present at these sites. SSA at the SGP and GVAX sites is similar (∼ 0.92 ± 0.04) and α is on the same order. On average, there was no significant difference in the magnitude of f_{RH} between these two sites where f_{RH} is generally large, indicating more hygroscopic particles present. NIM site has the lowest f_{RH} because dust aerosols

ACPD
13, 23023–23056, 2013

are primarily composed of insoluble components or components with low solubility. The mean number concentrations of CN and $CCN_{0.4}$ are small at the GRW site because there is less anthropogenic pollution, but the ratio of CCN to CN is high. This suggests that a large fraction of aerosol particles at this site can be activated into CCN. CN concentrations at the NIM site are the largest because dust events are rather frequent. The ability for dust particles to serve as CCN strongly depends on the amount of minor soluble substance (Rosenfeld et al., 2001; Kelly et al., 2007). CCN generally increases with CN during dust events, but the ratio of CCN to CN tends to decrease sharply with increasing CN, implying that less CCN become available under dusty conditions (J. Liu et al., 2011). This is why the smallest ratio of CCN to CN was found at the NIM site even though the $CCN_{0.4}$ concentration is moderately high.

3.1.1 Relationship between columnar aerosol optical quantities and CCN

For easy comparison with the result of Andreae (2009), the AOD-CCN relationships were obtained based on the function of $AOD = a \cdot (CCN_{0.4})^b$ (Andreae, 2009) for AOD at 440, 500, 675, 870 and 1020 nm. Figure 1 shows the relationship between $CCN_{0.4}$ and (a) AOD at 500 nm, (b) aerosol index (AI), and their corresponding correlation coefficients (R^2) (c and d) for different sites. AI is defined as the product of AOD at 500 nm and α (500–675 nm) to serve as a better proxy of CCN (Nakajima et al., 2001). The AOD and $CCN_{0.4}$ are well correlated in general with positive correlation, namely CCN increasing with AOD especially for the SGP, GVAX and FKB sites where the correlations are fairly good. Although the moderate correlation exists at the NIM site, the largest standard deviations and the smallest ratio of CCN to CN suggest that dust aerosols are not efficient CCN. They are, however, efficient in light scattering. In general, for most of the sites considered in this study, the correlation between AOD and CCN deteriorates with increasing wavelength. CCN is more closely correlated with AOD measurements at shorter wavelengths because the CCN concentration is dictated by fine-mode aerosols (Andreae, 2009). The relationship varies considerably from site

ACPD
13, 23023–23056, 2013

to site and thus large errors would incur if one global mean relationship is used, attesting to the need of different functions for different aerosol types/regions.

Both the ability of an aerosol particle to act as a CCN at a given super-saturation level and its contribution to extinction depends on the aerosol particle size distribution. Particle size is thus also a key factor influencing the AOD-CCN relationship. To assess this potential impact, Fig. 1b and d show the correlation between AI and CCN at 0.4 % supersaturation ($CCN_{0.4}$) at different wavelengths. Like AOD, CCN generally increases with the AI and the correlation is better than with the AOD at all sites. AI is more sensitive than AOD to the accumulation mode aerosol concentration, which is typically responsible for most CCN. Since α contains aerosol size information and AI conveys both aerosol loading and particle size information, the correlation between AI and CCN depends much weakly on the wavelength.

3.1.2 Relationship between in-situ aerosol optical quantities and CCN

Given that CCN is measured near the surface but that AOD denotes total light extinction in the whole atmospheric column, the AOD-CCN relationship must be affected by the vertical distribution of aerosols. To avoid such mismatch, Fig. 2 presents the same analysis results but using in-situ measurements of σ_{sp} at 450 nm in lieu of AOD (Fig. 2a) and the scattering aerosol index, Scat_AI (Fig. 2b). Figure 2c and d present correlation coefficients of the relationships between CCN and σ_{sp} (Fig. 2c) and the Scat_AI (Fig. 2d) for dry aerosol particles with $D_p \leq 1\,\mu m$. Scat_AI is the product of σ_{sp} and scattering wavelength exponent, α_{Scat}, which is expressed as

$$\alpha_{Scat} = -\log(\sigma_{sp,\lambda_1}/\sigma_{sp,\lambda_2})/\log(\lambda_1/\lambda_2)$$

Where σ_{sp,λ_1} and σ_{sp,λ_1} are scattering coefficients at wavelengths λ_1 and λ_2 (here, $\lambda_1 = 450\,nm$ and $\lambda_2 = 700\,nm$). At all sites, the correlations between σ_{sp} and CCN and Scat_AI and CCN are greater than those for the AOD-CCN and AI-CCN relationships (Fig. 1). The highest correlations are found for the Scat_AI-CCN relationships which also exhibits much less wavelength dependence.

ACPD
13, 23023–23056, 2013

The sound relationship between the aerosol optical quantities and CCN concentration indicates that if the vertical profile of aerosols scattering properties is known, the CCN profile may be estimated. It would be of great practical value to the study of aerosol indirect effects, as scattering is much more readily measured than CCN is. While this sounds encouraging, the uncertainty is rather large, up to a factor of two (Andreae, 2009). Accounting for some influential factors would help reduce the uncertainty.

3.2 Influence of ambient RH

The aerosol humidification effect is defined as the change in AOD in response to changing RH. For a hygroscopic particle, its size can be swelled by the uptake of water, which arguments the efficiency of scattering and thus increases its contribution to total extinction and AOD. On the other hand, its capability of being activated to become a CCN doesn't depend on RH for it is activated at super-saturation. This implies that changes in ambient RH can result in variations in AOD_{500} or AI even when $CCN_{0.4}$ concentrations remain the same. As such, the relationship between CCN and AOD or aerosol scattering coefficient is affected by RH, which is qualitatively investigated in the following way.

AOD and AI data originally averaged over different CCN concentration ranges were further binned within each CCN interval according to RH range (0–35 %, 35–75 %, and 75–100 %). Figure 3 shows AOD and AI as a function of CCN concentration for these different RH bins using data from the SGP site. Both AOD_{500} and AI increase with increasing ambient RH within the same ranges of $CCN_{0.4}$ concentration. The correlation between AOD_{500} and CCN concentration becomes weak when ambient RH values are above 75 % due to the strong aerosol swelling effect on AOD_{500} (Jeong et al., 2007). The increase in particle size implies that α decreases, which has been demonstrated by others (Noh et al., 2011). This increase in AOD and decrease in α with increasing RH complicates the relationship between AI and $CCN_{0.4}$. Unless RH is very high, e.g., greater than 95 %, changes in humidity do not influence the wavelength dependence

ACPD
13, 23023–23056, 2013

of scattering in any significant way because scattering coefficients at all wavelengths change by similar factors and absorption is usually a minor fraction of extinction (Shinozuka et al., 2007). AOD_{500} or AI values under lower ambient RH conditions are more representative of the real effects of aerosol.

Figure 4 shows the correlation coefficients of the relationships between in-situ σ_{sp} and CCN for aerosol particles with $D_p \leq 1\,\mu m$ and at ambient RH conditions as a function of wavelength at all sites. The correlation coefficients of σ_{sp}-CCN relationships at ambient RH levels are generally lower than those under dry RH conditions (Fig. 2c). For example, at GRW site, relative to dry condition, R^2 at ambient condition decreased by 13.8 %, 21.8 % and 31.6 % at 450, 550 and 700 nm, respectively. Here, the percentage decrease is calculated as $(R^2_{amb} - R^2_{dry})/R^2_{dry} \times 100\,\%$, where R^2_{amb} and R^2_{dry} are correlation coefficients σ_{sp} at ambient conditions and dry conditions, respectively. The σ_{sp}-CCN relationship at the NIM site is least affected by RH because RH is low in that region and the prevalent dust aerosols have a relatively low hygroscopicity. These results suggest that the influence of RH on the relationship between aerosol optical quantities and CCN concentration needs to be taken into consideration unless AOD is measured at low and/or constant ambient RH conditions.

3.3 Influence of aerosol hygroscopicity

As per the above, hygroscopicity and RH jointly determine the swelling effect which affect AOD and σ_{sp} and thus the AOD (σ_{sp})-CCN relationships. Having addressed the effect of RH, the hygroscopicity is investigated by minimizing the influence of ambient RH using in-situ measurements of σ_{sp} under a fixed moderately dry condition ($\sim 40\,\%$). Figure 5 shows σ_{sp}-$CCN_{0.4}$ relationship for different ranges of f_{RH} for dry aerosol particles with $D_p \leq 1\,\mu m$ (Fig. 5a) and $D_p \leq 10\,\mu m$ (Fig. 5b) at the SGP. No clear influence is seen of f_{RH} on any σ_{sp}-CCN for dry particles with $D_p \leq 1\,\mu m$ and $D_p \leq 10\,\mu m$.

The f_{RH} significantly dependent on the aerosol chemical composition and can be considered as an agent of chemical composition (Jeong et al., 2007; P. F. Liu et al., 2011). It also conveys information about the ability of aerosol light scattering/extinction

ACPD
13, 23023–23056, 2013

enhancement with the increasing RH. Fundamentally, if aerosol particles are highly hygroscopic, they should be more readily to be activated into CCN. To further see the influence of f_{RH} on σ_{sp}-CCN relationship, the CCN concentration and σ_{sp} at 450 nm for dry particles with $D_p \leq 1\,\mu m$ (Fig. 6a) and the ratio of CCN to σ_{sp} (Fig. 6b) as a function of f_{RH} are plotted. No significantly changes on CCN and σ_{sp} with increasing of f_{RH} are found, especially in the range of f_{RH} larger than 1.5 (Fig. 6a). Since there is no significantly variation of CCN and σ_{sp} with changes of f_{RH}, the ratio of CCN to scattering coefficients shows the insensitivity to increasing f_{RH}. They support the finding that f_{RH} has weak influence on σ_{sp}-CCN relationship. Also, the scattering wavelength exponent in each f_{RH} is 1.69 ± 0.40, 1.67 ± 0.40, 1.70 ± 0.40 and 1.76 ± 0.34, respectively, which shows almost no changes with variation of f_{RH}.

It is still unclear how useful is the growth characteristics as denoted by f_{RH} for inferring CCN properties (Ervens et al., 2007). Studies have shown that the most important piece of information for CCN closure is the aerosol size distribution followed by aerosol composition (Dusek et al., 2006), both affecting aerosol hygroscopicity (Ervens et al., 2007). This is probably because natural aerosols are readily mixed well enough so that differences in their composition may not standout clearly as their signal may be weaker than the uncertainties resulting from the measurements of pertinent variables.

3.4 Influence of aerosol SSA

In addition to AOD and the Angstrom exponent that measure aerosol loading and size, aerosol SSA, defined as the ratio of scattering to extinction, is another independent aerosol attribute denoting aerosol composition and size and thus potentially affect CCN-AOD (σ_{sp}) relationship. SSA can be estimated from surface measurements by a scanning sunphotometer such as those under the AERONET (Dubovik and King, 2000), combination of direct-beam and diffuse radiation (Zhao and Li, 2007), or a combination of surface-measured total attenuation and satellite-measured atmospheric reflection (Lee et al., 2007). Since both AOD and SSA are influenced by ambient RH, only surface measured σ_{sp} and SSA at fixed RH ($\sim = 40\,\%$) are used here to eliminate

ACPD
13, 23023–23056, 2013

the influence of ambient RH. Figure 7 shows σ_{sp}-$CCN_{0.4}$ for different ranges of SSA at 450 nm with $D_p \leq 1$ µm. σ_{sp} generally increases with increasing SSA for the same ranges of $CCN_{0.4}$ concentration. Low SSA values are generally associated with high CCN concentrations, while high SSA values are associated with lower CCN concentrations.

Figure 8a plots the variations of $CCN_{0.4}$ concentration, σ_{sp} and their radio (CCN/σ_{sp}) at 450 nm for $D_p \leq 1$ µm. $CCN_{0.4}$ concentrations slightly decrease with increasing SSA, while σ_{sp} increases significantly with increasing SSA. Thus, their ratio shows a significant decrease with increasing SSA. The dependences may be driven by various mechanisms. One has to do with a polluted air mass containing light-absorbing soot particles coated with volatile material (e.g., sulfate and organic) (Clarke et al., 2007) that are efficient CCN, but inefficient scatter. Therefore, they enhance CCN but lower SSA (Shinozuka, 2008). As they age, the particles grow in size due to deposition of soluble mass, such as sulfate and nitrate, so can then scatter more, while their number concentration remains constant or decreases due to coagulation (Shinozuka, 2008). To constrain any influence of particle size which also affects CCN and aerosol optical quantities, the same relationships are plotted in Fig. 8b with a narrow range of the Angstrom exponent between 1.6 and 1.8. Similar trends are found, eliminating the cause of particle size as a driving force behind the relationships.

Results presented here suggest that SSA has a significant influence on the relationship between CCN concentration and aerosol optical quantities and if used as a constraint, may reduce uncertainties in the relationship. Similar results were reported by Shinozuka (2008), who showed that, using SSA as a constraint, the estimation of CCN concentration from aerosol extinction coefficients for pollution particles in Mexico is improved by up to 20–30 %.

3.5 Parameterizations for estimating CCN

Instead of using a conventional fixed AOD-CCN relationship, the above analyses help us develop more accurate relationships by accounting for the major influential factors

ACPD
13, 23023–23056, 2013

to improve the estimation of CCN with variable amount of information on the influential factors. A relationship between CCN and AOD is first developed by considering the influences of particle size and aerosol SSA. While we demonstrate the strong influence of RH, correcting for this effect cannot be generalized for it depends on aerosol type. On the other hand, the swelling effect is only significant for large RH (>90 %). We would thus leave the correction for this effect to the users who can do it based on measured function of f_{RH}. Here, we limit our parameterization to RH<80 %, i.e. only measurements made under dry to modest moist conditions are used here. The large dataset from ARM SGP allows us to develop the parameterization that may be valid for other rural continental regions.

The parameterization is given as:

$$CCN_{0.4} = 1.2824e^{5} \cdot \left[AOD_{500} \cdot \alpha\right]^{2.3941} \quad 0.85 < SSA < 0.95 \tag{5}$$

R^2 is 0.94 and the mean relative error (RE), defined as $(CCN_C\text{-}CCN_M)/CCN_M$ is 0.85. Here, CCN_C and CCN_M is calculated CCN concentration using above equation and measured CCN concentration, respectively. SSA is limited to 0.85 to 0.95, which represents most of aerosol particles with moderate scattering and absorbing properties.

The relatively large error mainly attributes to the fact that CCN is measured near the surface but AOD denotes total light extinction in the whole atmospheric column, let alone the unaccounted swelling effect which may not be very large due to the constraint in RH. Compared to the use of a single fixed relationship between CCN and AOD, R^2 is improved by 9.3 % (0.94 vs. 0.86) and RE is improved about 11.5 % (0.85 vs. 0.96).

If there are in-situ aerosol optical measurements such as σ_{sp}, estimation of CCN can be improved by the following parameterization:

$$CCN_{0.4} = 2.3397 \cdot \left[\sigma_{sp} \cdot \alpha\right]^{1.5178} \quad 0.85 < SSA < 0.95 \tag{6}$$

R^2 is improved from 0.94 to 0.99 and mean RE is reduced from 0.85 to 0.20, relative to Eq. (5). Relative to a single fixed CCN-σ_{sp} relationship without accounting any influ-

ACPD
13, 23023–23056, 2013

ential factors, R^2 of Eq. (6) does not differ considerably (0.99 vs. 0.97); the mean RE is significantly decreased by as much as 74.7 % (0.20 vs. 0.79).

4 Summary and conclusions

Due to the dearth of CCN measurements, aerosol loading has often been used as a proxy or predictor of CCN in large-scale applications such as GCM modeling. Based on extensive measurements of aerosol optical quantities and CCN number concentration made at different Atmospheric Radiation Measurement (ARM) Climate Research Facility sites, the relationships between aerosol optical quantities, including columnar AOD, surface-measured aerosol scattering parameters, and CCN concentrations are assessed. For the purpose of constraining and reducing the variability and uncertainties in relating aerosol optical quantities and CCN concentration, the influences of RH, aerosol hygroscopicity and SSA are investigated using more extensive routine observations at the ARM permanent site over the South Great Plains (SGP) site.

In general, mean AOD-CCN relationships at the SGP, GVAX and FKB sites show a variable degree of correlation. Weaker correlation is found at the GRW and NIM sites where relatively large particles dominate. In general, the correlation decreases as the wavelength at which AOD is measured increases. It is thus recommended to use AOD values measured at the shortest wavelengths. Moreover, it is better to use aerosol index (AI) derived from AOD measurements at two wavelengths than AOD at a single wavelength, as the relationship between AI and CCN is systematically better than the CCN-AOD relation. The best predictors of CCN are in-situ aerosol scattering (also extinction) coefficient and aerosol indices measured simultaneously with CCN.

AOD and AI are significantly influenced by ambient RH levels. The correlation between AOD (AI) and CCN becomes weak when ambient RH values are high, e.g., greater than 75 %, due to the strong aerosol swelling effects on AOD. The correlation between aerosol optical quantities and CCN concentration is much tighter for dry air than for humid air. This implies that aerosol optical quantities measured at low RH are

ACPD
13, 23023–23056, 2013

better representative of the real effects due to aerosols. No significant influence of the aerosol hygroscopic growth factor on any CCN-σ_{sp} relationship is found. Particles with low SSA are generally associated with higher CCN concentrations for the same scattering coefficient and lower σ_{sp} values. Aerosol single scattering albedo (SSA) is found to have a significant influence on the relationship between CCN concentration and aerosol optical quantities and if used as a constraint, can reduce uncertainties in the estimate of CCN. Note that both f_{RH} and SSA are related with aerosol chemical compositions, but are concerned with different aerosol properties. Our finding suggests that the CCN-σ_{sp} relationship is more sensitive to the composition of matter to absorption than to hydroscopcity. This appears to concur the finding that the impact of composition CCN is secondary while SSA dictates more strongly on extinction and scattering.

To improve the accuracy of CCN estimation, some influential factors are accounted for in developing parameterization schemes for estimating CCN from aerosol optical quantities, AOD, Angstrom exponent, in-situ aerosol scattering coefficient. The best results are achieved by using aerosol scattering coefficients and SSA, and the worst is the use of a fixed AOD-CCN relationship. To avoid the swelling effect, the parameterization is valid for RH < 80 %. If the humidification function and humidity are known, one can correct for the effect.

This study reveals the potentials and limitations of using aerosol optical property measurements to infer CCN concentration with a focus on the impact of ambient RH, aerosol hygroscopic response, and SSA. Further evaluation and analyses will require aerosol composition and aerosol size distribution information, together with aerosol optical parameters and meteorological parameters for each aerosol type and region.

4.1 Acknowledgements.

Acknowledgements. Data were obtained from the Atmospheric Radiation Measurement (ARM) Program sponsored by the US Department of Energy, Office of Science, Office of Biological and Environmental Research, Climate and Environmental Sciences Division. AOD values were obtained from the AERONET database at http://aeronet.gsfc.nasa.gov. This study has been

ACPD
13, 23023–23056, 2013

supported by the National Basic Research Program (2013CB955804), National Science Foundation (1118325) and Department of Energy's Atmospheric System Research (ER65319).

References

Alexander, D. T. L., Crozier, P. A., and Anderson, J. R.: Brown Carbon Spheres in East Asian Outflow and Their Optical Properties, Science, 321, 833–836, 2008.

Anderson, B. E., Grant, W. B., Gregory, G. L., Browell, E. V., Collins, J. E., Jr., Sachse, G. W., Bagwell, D. R., Hudgins, C. H., Blake, D. R., and Blake, N. J.: Aerosols from biomass burning over the tropical South Atlantic region: Distributions and impacts, J. Geophys. Res., 101, 24117–24137, doi:10.1029/96jd00717, 1996.

Andreae, M. O.: Correlation between cloud condensation nuclei concentration and aerosol optical thickness in remote and polluted regions, Atmos. Chem. Phys., 9, 543–556, doi:10.5194/acp-9-543-2009, 2009.

Andreae, M. O. and Rosenfeld, D.: Aerosol-cloud-precipitation interactions. Part 1. The nature and sources of cloud-active aerosols, Earth-Sci. Rev., 89, 13–41, 2008.

Andreae, M. O., Rosenfeld, D., Artaxo, P., Costa, A. A., Frank, G. P., Longo, K. M., and Silva-Dias, M. A. F.: Smoking Rain Clouds over the Amazon, Science, 303, 1337–1342, 2004.

Bell, T. L., Rosenfeld, D., Kim, K.-M., Yoo, J.-M., Lee, M.-I., and Hahnenberger, M.: Midweek increase in U.S. summer rain and storm heights suggests air pollution invigorates rainstorms, J. Geophys. Res., 113, D02209, doi:10.1029/2007jd008623, 2008.

Bréon, F.-M., Tanré, D., and Generoso, S.: Aerosol Effect on Cloud Droplet Size Monitored from Satellite, Science, 295, 834–838, 2002.

Clarke, A., McNaughton, C., Kapustin, V., Shinozuka, Y., Howell, S., Dibb, J., Zhou, J., Anderson, B., Brekhovskikh, V., Turner, H., and Pinkerton, M.: Biomass burning and pollution aerosol over North America: Organic components and their influence on spectral optical properties and humidification response, J. Geophys. Res., 112, D12S18, doi:10.1029/2006jd007777, 2007.

Dubovik, O. and King, M. D.: A flexible inversion algorithm for retrieval of aerosol optical properties from sun and sky radiance measurements, J. Geophys. Res., 105, 20673–20696, 2000.

Dusek, U., Frank, G. P., Hildebrandt, L., Curtius, J., Schneider, J., Walter, S., Chand, D., Drewnick, F., Hings, S., Jung, D., Borrmann, S., and Andreae, M. O.: Size Matters More

ACPD
13, 23023–23056, 2013

Than Chemistry for Cloud-Nucleating Ability of Aerosol Particles, Science, 312, 1375–1378, 2006.
Ervens, B., Cubison, M., Andrews, E., Feingold, G., Ogren, J. A., Jimenez, J. L., DeCarlo, P., and Nenes, A.: Prediction of cloud condensation nucleus number concentration using measurements of aerosol size distributions and composition and light scattering enhancement due to humidity, J. Geophys. Res., 112, D10S32, doi:10.1029/2006jd007426, 2007.
Facchini, M. C., Mircea, M., Fuzzi, S., and Charlson, R. J.: Cloud albedo enhancement by surface-active organic solutes in growing droplets, Nature, 401, 257–259, 1999.
Feingold, G., Eberhard, W. L., Veron, D. E., and Previdi, M.: First measurements of the Twomey indirect effect using ground-based remote sensors, Geophys. Res. Lett., 30, 1287, doi:10.1029/2002gl016633, 2003.
Ghan, S. J. and Collins, D. R.: Use of In Situ Data to Test a Raman Lidar–Based Cloud Condensation Nuclei Remote Sensing Method, J. Atmos. Ocean. Tech., 21, 387–394, 2004.
Ghan, S. J., Rissman, T. A., Elleman, R., Ferrare, R. A., Turner, D., Flynn, C., Wang, J., Ogren, J., Hudson, J., Jonsson, H. H., VanReken, T., Flagan, R. C., and Seinfeld, J. H.: Use of in situ cloud condensation nuclei, extinction, and aerosol size distribution measurements to test a method for retrieving cloud condensation nuclei profiles from surface measurements, J. Geophys. Res., 111, D05S10, doi:10.1029/2004jd005752, 2006.
Grandey, B. S., Stier, P., and Wagner, T. M.: Investigating relationships between aerosol optical depth and cloud fraction using satellite, aerosol reanalysis and general circulation model data, Atmos. Chem. Phys., 13, 3177–3184, doi:10.5194/acp-13-3177-2013, 2013.
Heintzenberg, J., Wiedensohler, A., Tuch, T. M., Covert, D. S., Sheridan, P., Ogren, J. A., Gras, J., Nessler, R., Kleefeld, C., Kalivitis, N., Aaltonen, V., Wilhelm, R. T., and Havlicek, M.: Intercomparisons and Aerosol Calibrations of 12 Commercial Integrating Nephelometers of Three Manufacturers, J. Atmos. Ocean. Tech., 23, 902–914, doi:10.1175/jtech1892.1, 2006.
Holben, B. N., Eck, T. F., Slutsker, I., Tanré, D., Buis, J. P., Setzer, A., Vermote, E., Reagan, J. A., Kaufman, Y. J., Nakajima, T., Lavenu, F., Jankowiak, I., and Smirnov, A.: AERONET—A Federated Instrument Network and Data Archive for Aerosol Characterization, Remote Sens. Environ., 66, 1–16, 1998.
Hudson, J. G. and Yum, S. S.: Cloud condensation nuclei spectra and polluted and clean clouds over the Indian Ocean, J. Geophys. Res., 107, 8022, doi:10.1029/2001jd000829, 2002.

ACPD
13, 23023–23056, 2013

IPCC: Climate Change 2007: The Physical Science Basis. Contribution of Working Group I to the Fourth Assessment Report of the Intergovernmental Panel on Climate Change, Cambridge University Press, Cambridge, United Kingdom and New York, NY, USA, 2007.
Jefferson, A.: Aerosol Observing System (AOS) Handbook, ARMTR-014, US Dep. Of Energy, Washington, D.C., 2005.
Jefferson, A.: Empirical estimates of CCN from aerosol optical properties at four remote sites, Atmos. Chem. Phys., 10, 6855–6861, doi:10.5194/acp-10-6855-2010, 2010.
Jeong, M.-J., Li, Z., Andrews, E., and Tsay, S.-C.: Effect of aerosol humidification on the column aerosol optical thickness over the Atmospheric Radiation Measurement Southern Great Plains site, J. Geophys. Res., 112, D10202, doi:10.1029/2006jd007176, 2007.
Ji, Q. and Shaw, G. E.: On supersaturation spectrum and size distributions of cloud condensation nuclei, Geophys. Res. Lett., 25, 1903–1906, 1998.
Kanakidou, M., Seinfeld, J. H., Pandis, S. N., Barnes, I., Dentener, F. J., Facchini, M. C., Van Dingenen, R., Ervens, B., Nenes, A., Nielsen, C. J., Swietlicki, E., Putaud, J. P., Balkanski, Y., Fuzzi, S., Horth, J., Moortgat, G. K., Winterhalter, R., Myhre, C. E. L., Tsigaridis, K., Vignati, E., Stephanou, E. G., and Wilson, J.: Organic aerosol and global climate modelling: a review, Atmos. Chem. Phys., 5, 1053–1123, doi:10.5194/acp-5-1053-2005, 2005.
Kapustin, V. N., Clarke, A. D., Shinozuka, Y., Howell, S., Brekhovskikh, V., Nakajima, T., and Higurashi, A.: On the determination of a cloud condensation nuclei from satellite: Challenges and possibilities, J. Geophys. Res., 111, D04202, doi:10.1029/2004jd005527, 2006.
Kelly, J. T., Chuang, C. C., and Wexler, A. S.: Influence of dust composition on cloud droplet formation, Atmos. Environ., 41, 2904–2916, 2007.
Koren, I., Kaufman, Y. J., Rosenfeld, D., Remer, L. A., and Rudich, Y.: Aerosol invigoration and restructuring of Atlantic convective clouds, Geophys. Res. Lett., 32, L14828, doi:10.1029/2005gl023187, 2005.
Koren, I., Martins, J. V., Remer, L. A., and Afargan, H.: Smoke Invigoration Versus Inhibition of Clouds over the Amazon, Science, 321, 946–949, doi:10.1126/science.1159185, 2008.
Koren, I., Feingold, G., and Remer, L. A.: The invigoration of deep convective clouds over the Atlantic: aerosol effect, meteorology or retrieval artifact?, Atmos. Chem. Phys., 10, 8855–8872, doi:10.5194/acp-10-8855-2010, 2010.
Lee, K. H., Li, Z., Wong, M. S., Xin, J., Wang, Y., Hao, W.-M., and Zhao, F.: Aerosol single scattering albedo estimated across China from a combination of ground and satellite measurements, J. Geophys. Res., 112, D22S15, doi:10.1029/2007jd009077, 2007.

ACPD
13, 23023–23056, 2013

Li, Z., Niu, F., Fan, J., Liu, Y., Rosenfeld, D., and Ding, Y.: Long-term impacts of aerosols on the vertical development of clouds and precipitation, Nat. Geosci., 4, 888–894, 2011.
Lin, J. C., Matsui, T., Pielke, R. A., and Kummerow, C.: Effects of biomass-burning-derived aerosols on precipitation and clouds in the Amazon Basin: a satellite-based empirical study, J. Geophys. Res., 111, D19204, doi:10.1029/2005jd006884, 2006.
Liu, J., Zheng, Y., Li, Z., and Cribb, M.: Analysis of cloud condensation nuclei properties at a polluted site in southeastern China during the AMF-China Campaign, J. Geophys. Res., 116, D00K35, doi:10.1029/2011jd016395, 2011.
Liu, J., Zheng, Y., Li, Z., Flynn, C., and Cribb, M.: Seasonal variations of aerosol optical properties, vertical distribution and associated radiative effects in the Yangtze Delta region of China, J. Geophys. Res., 117, D00K38, doi:10.1029/2011jd016490, 2012.
Liu, P. F., Zhao, C. S., Göbel, T., Hallbauer, E., Nowak, A., Ran, L., Xu, W. Y., Deng, Z. Z., Ma, N., Mildenberger, K., Henning, S., Stratmann, F., and Wiedensohler, A.: Hygroscopic properties of aerosol particles at high relative humidity and their diurnal variations in the North China Plain, Atmos. Chem. Phys., 11, 3479–3494, doi:10.5194/acp-11-3479-2011, 2011.
McFiggans, G., Artaxo, P., Baltensperger, U., Coe, H., Facchini, M. C., Feingold, G., Fuzzi, S., Gysel, M., Laaksonen, A., Lohmann, U., Mentel, T. F., Murphy, D. M., O'Dowd, C. D., Snider, J. R., and Weingartner, E.: The effect of physical and chemical aerosol properties on warm cloud droplet activation, Atmos. Chem. Phys., 6, 2593–2649, doi:10.5194/acp-6-2593-2006, 2006.
Nakajima, T.: A possible correlation between satellite-derived cloud and aerosol microphysical parameters, Geophys. Res. Lett., 28, 1171–1174, 2001.
Niu, Feng and Li, Zhanqing: Systematic variations of cloud top temperature and precipitation rate with aerosols over the global tropics, Atmos. Chem. Phys., 12, 8491–8498, doi:10.5194/acp-12-8491-2012, 2012.
Noh, Y. M., Müller, D., Mattis, I., Lee, H., and Kim, Y. J.: Vertically resolved light-absorption characteristics and the influence of relative humidity on particle properties: Multiwavelength Raman lidar observations of East Asian aerosol types over Korea, J. Geophys. Res., 116, D06206, doi:10.1029/2010jd014873, 2011.
Orville, R. E., Huffines, G., Nielsen-Gammon, J., Zhang, R., Ely, B., Steiger, S., Phillips, S., Allen, S., and Read, W.: Enhancement of cloud-to-ground lightning over Houston, Texas, Geophys. Res. Lett., 28, 2597–2600, doi:10.1029/2001gl012990, 2001.

ACPD
13, 23023–23056, 2013

Petters, M. D. and Kreidenweis, S. M.: A single parameter representation of hygroscopic growth and cloud condensation nucleus activity, Atmos. Chem. Phys., 7, 1961–1971, doi:10.5194/acp-7-1961-2007, 2007.

Quaas, J., Ming, Y., Menon, S., Takemura, T., Wang, M., Penner, J. E., Gettelman, A., Lohmann, U., Bellouin, N., Boucher, O., Sayer, A. M., Thomas, G. E., McComiskey, A., Feingold, G., Hoose, C., Kristjánsson, J. E., Liu, X., Balkanski, Y., Donner, L. J., Ginoux, P. A., Stier, P., Grandey, B., Feichter, J., Sednev, I., Bauer, S. E., Koch, D., Grainger, R. G., Kirkevåg, A., Iversen, T., Seland, Ø., Easter, R., Ghan, S. J., Rasch, P. J., Morrison, H., Lamarque, J.-F., Iacono, M. J., Kinne, S., and Schulz, M.: Aerosol indirect effects – general circulation model intercomparison and evaluation with satellite data, Atmos. Chem. Phys., 9, 8697–8717, doi:10.5194/acp-9-8697-2009, 2009.

Ramanathan, V., Crutzen, P. J., Kiehl, J. T., and Rosenfeld, D.: Aerosols, Climate, and the Hydrological Cycle, Science, 294, 2119–2124, doi:10.1126/science.1064034, 2001.

Roberts, G. C. and Nenes, A.: A Continuous-Flow Streamwise Thermal-Gradient CCN Chamber for Atmospheric Measurements, Aerosol Sci. Tech., 39, 206–221, doi:10.1080/027868290913988, 2005.

Rose, D., Gunthe, S. S., Mikhailov, E., Frank, G. P., Dusek, U., Andreae, M. O., and Pöschl, U.: Calibration and measurement uncertainties of a continuous-flow cloud condensation nuclei counter (DMT-CCNC): CCN activation of ammonium sulfate and sodium chloride aerosol particles in theory and experiment, Atmos. Chem. Phys., 8, 1153–1179, doi:10.5194/acp-8-1153-2008, 2008.

Rosenfeld, D. and Woodley, W. L.: Deep convective clouds with sustained supercooled liquid water down to −37.5 °C, Nature, 405, 440–442, 2000.

Rosenfeld, D., Rudich, Y., and Lahav, R.: Desert dust suppressing precipitation: A possible desertification feedback loop, P. Natl. Acad. Sci. USA, 98, 5975–5980, 2001.

Ross, K. E., Piketh, S. J., Bruintjes, R. T., Burger, R. P., Swap, R. J., and Annegarn, H. J.: Spatial and seasonal variations in CCN distribution and the aerosol-CCN relationship over southern Africa, J. Geophys. Res., 108, 8481, doi:10.1029/2002jd002384, 2003.

Shinozuka, Y.: Relations between cloud condensation nuclei and aerosol optical properties relevant to remote sensing, Ph.D. thesis, Dep. of Ocean and Earth Science and Technology, University of Hawaii at Manoa, Hawaii, US, 2008.

Shinozuka, Y., Clarke, A. D., Howell, S. G., Kapustin, V. N., McNaughton, C. S., Zhou, J., and Anderson, B. E.: Aircraft profiles of aerosol microphysics and optical properties over North

ACPD
13, 23023–23056, 2013

America: Aerosol optical depth and its association with $PM_{2.5}$ and water uptake, J. Geophys. Res., 112, D12S20, doi:10.1029/2006jd007918, 2007.
Shinozuka, Y., Clarke, A. D., DeCarlo, P. F., Jimenez, J. L., Dunlea, E. J., Roberts, G. C., Tomlinson, J. M., Collins, D. R., Howell, S. G., Kapustin, V. N., McNaughton, C. S., and Zhou, J.: Aerosol optical properties relevant to regional remote sensing of CCN activity and links to their organic mass fraction: airborne observations over Central Mexico and the US West Coast during MILAGRO/INTEX-B, Atmos. Chem. Phys., 9, 6727–6742, doi:10.5194/acp-9-6727-2009, 2009.
Shulman, M. L., Jacobson, M. C., Carlson, R. J., Synovec, R. E., and Young, T. E.: Dissolution behavior and surface tension effects of organic compounds in nucleating cloud droplets, Geophys. Res. Lett., 23, 277–280, doi:10.1029/95gl03810, 1996.
Steiger, S. M. and Orville, R. E.: Cloud-to-ground lightning enhancement over Southern Louisiana, Geophys. Res. Lett., 30, 1975, doi:10.1029/2003gl017923, 2003.
Svenningsson, B., Rissler, J., Swietlicki, E., Mircea, M., Bilde, M., Facchini, M. C., Decesari, S., Fuzzi, S., Zhou, J., Mønster, J., and Rosenørn, T.: Hygroscopic growth and critical supersaturations for mixed aerosol particles of inorganic and organic compounds of atmospheric relevance, Atmos. Chem. Phys., 6, 1937–1952, doi:10.5194/acp-6-1937-2006, 2006.
Tao, W.-K., Chen, J.-P., Li, Z., Wang, C., and Zhang, C.: Impact of aerosols on convective clouds and precipitation, Rev. Geophys., 50, RG2001, doi:10.1029/2011rg000369, 2012.
Twomey, S.: The nuclei of natural cloud formation part II: The supersaturation in natural clouds and the variation of cloud droplet concentration, Pure Appl. Geophys., 43, 243–249, 1959.
Twomey, S.: The Influence of Pollution on the Shortwave Albedo of Clouds, J. Atmos. Sci., 34, 1149–1152, 1977.
Twomey, S. A., Piepgrass, M., and Wolfe, T. L.: An assessment of the impact of pollution on global cloud albedo, Tellus B, 36B, 356–366, doi:10.1111/j.1600-0889.1984.tb00254.x, 1984.
Wang, M., Ghan, S., Ovchinnikov, M., Liu, X., Easter, R., Kassianov, E., Qian, Y., and Morrison, H.: Aerosol indirect effects in a multi-scale aerosol-climate model PNNL-MMF, Atmos. Chem. Phys., 11, 5431–5455, doi:10.5194/acp-11-5431-2011, 2011.
Ward, D. S., Eidhammer, T., Cotton, W. R., and Kreidenweis, S. M.: The role of the particle size distribution in assessing aerosol composition effects on simulated droplet activation, Atmos. Chem. Phys., 10, 5435–5447, doi:10.5194/acp-10-5435-2010, 2010.

ACPD
13, 23023–23056, 2013

Yang, F., Xue, H., Deng, Z., Zhao, C., and Zhang, Q.: A closure study of cloud condensation nuclei in the North China Plain using droplet kinetic condensational growth model, Atmos. Chem. Phys., 12, 5399–5411, doi:10.5194/acp-12-5399-2012, 2012.

Yang, X., Yao, Z., Li, Z., and Fan, T.: Heavy air pollution suppresses summer thunderstorms in central China, J. Atmos. Sol-Terr. Phy., 95–96, 28–40, 2013.

Yuan, T., Li, Z., Zhang, R., and Fan, J.: Increase of cloud droplet size with aerosol optical depth: an observation and modeling study, J. Geophys. Res., 113, D04201, doi:10.1029/2007JD008632, 2008.

Yuan, T., Remer, L. A., Pickering, K. E., and Yu, H.: Observational evidence of aerosol enhancement of lightning activity and convective invigoration, Geophys. Res. Lett., 38, L04701, doi:10.1029/2010gl046052, 2011.

Yum, S. S., Roberts, G., Kim, J. H., Song, K., and Kim, D.: Submicron aerosol size distributions and cloud condensation nuclei concentrations measured at Gosan, Korea, during the Atmospheric Brown Clouds & East Asian Regional Experiment 2005, J. Geophys. Res., 112, D22S32, doi:10.1029/2006jd008212, 2007.

Zhang, Q., Jimenez, J. L., Canagaratna, M. R., Allan, J. D., Coe, H., Ulbrich, I., Alfarra, M. R., Takami, A., Middlebrook, A. M., Sun, Y. L., Dzepina, K., Dunlea, E., Docherty, K., DeCarlo, P. F., Salcedo, D., Onasch, T., Jayne, J. T., Miyoshi, T., Shimono, A., Hatakeyama, S., Takegawa, N., Kondo, Y., Schneider, J., Drewnick, F., Borrmann, S., Weimer, S., Demerjian, K., Williams, P., Bower, K., Bahreini, R., Cottrell, L., Griffin, R. J., Rautiainen, J., Sun, J. Y., Zhang, Y. M., and Worsnop, D. R.: Ubiquity and dominance of oxygenated species in organic aerosols in anthropogenically-influenced Northern Hemisphere midlatitudes, Geophys. Res. Lett., 34, L13801, doi:10.1029/2007gl029979, 2007.

Zhao, F. and Li, Z.: Estimation of aerosol single scattering albedo from solar direct spectral radiance and total broadband irradiances measured in China, J. Geophys. Res., 112, 1–10, 2007.

ACPD
13, 23023–23056, 2013

Table 1. Description of ARM[1] data sets selected for this study.

Site[2]	Location/Altitude	Time Range	Environment	Measurements used in the study
SGP	36.6° N; 97.5° W/320 m	2006.09–2011.04	Agriculture	AOD[3] and α[4] from AERONET[5] measurements
GRW	39.1° N; 28.0° W/15 m	2009.05–2010.12	Marine	CCN[6], CN[7], $\sigma_{sp}(\sigma_{ap})$[8], SSA[9], $f^{10}_{RH(RH/RH_{Ref})}$
NIM	13.5° N; 2.2° E/205 m	2006.08–2007.01	Dust region	from ground-based AOS[11]
GVAX	29.4° N; 79.5° E/1936 m	2011.06–2012.04	Industrial emission and biomass burning	Atmospheric RH from Surface Meteorological Instrumentation
FKB	48.5° N; 8.4° E/511 m	2007.04–2007.12	Forest	

[1] ARM-Atmospheric Radiation Measurement; [2] SGP-Southern Great Plains, USA; GRW-Graciosa Island, Azores; NIM-Niamey, Niger, West Africa; GVAX-Ganges Valley Aerosol Experiment, Ganges Valley region of India; FKB-Black Forest region, Germany; [3] AOD-Aerosol Optical Depth; [4] α-Angstrom Wavelength Exponent; [5] AERONET-Aerosol Robotic Network; [6] CCN-Cloud Condensation Nuclei; [7] CN-Condensation Nuclei; [8] σ_{sp}-Aerosol light scattering coefficients; σ_{ap}-Aerosol light absorption coefficients; [9] SSA-Single Scattering Albedo, equal to the ratio of σ_{sp} to $(\sigma_{sp} + \sigma_{ap})$; [10] $f_{RH(RH/RH_{Ref})}$-Aerosol hygroscopic growth factor defined as the ratio of σ_{sp} at a given RH to σ_{sp} at a low reference RH; [11] AOS-Aerosol Observing System, the primary ARM platform for in situ aerosol measurements made at the surface.

ACPD
13, 23023–23056, 2013

Table 2. Summary of mean aerosol optical quantities, CN concentration, and CCN concentration at 0.4 % supersaturation during the study period.

Sites	AOD 500 nm	α500–675 nm;	σ_{sp}	SSA 450 nm	f_{RH}450 nm	CN [cm^{-3}]	CCN$_{0.4}$[cm^{-3}]	CCN/CN 0.4 S
SGP	0.10 ± 0.08	1.28 ± 0.34	41.8 ± 34.1 ($D_p \leq 1$ µm) 50.5 ± 44.8 ($D_p \leq 10$ µm)	0.92 ± 0.05 ($D_p \leq 1$ µm) 0.92 ± 0.05 ($D_p \leq 10$ µm)	1.54 ± 0.28 ($D_p \leq 1$ µm) 1.52 ± 0.28 ($D_p \leq 10$ µm)	3944 ± 2992	1248 ± 896	0.40 ± 0.24
GRW	0.11 ± 0.06	0.75 ± 0.35	7.7 ± 7.7 ($D_p \leq 1$ µm) 22.8 ± 16.5 ($D_p \leq 10$ µm)	0.91 ± 0.06 ($D_p \leq 1$ µm) 0.93 ± 0.04 ($D_p \leq 10$ µm)	1.31 ± 0.24 ($D_p \leq 1$ µm) 1.36 ± 0.21 ($D_p \leq 10$ µm)	615 ± 587	287 ± 263	0.53 ± 0.30
NIM	0.39 ± 0.33	0.47 ± 0.23	54.6 ± 98.8 ($D_p \leq 1$ µm) 106.2 ± 200.7 ($D_p \leq 10$ µm)	0.81 ± 0.07 ($D_p \leq 1$ µm) 0.82 ± 0.06 ($D_p \leq 10$ µm)	1.18 ± 0.11 ($D_p \leq 1$ µm) 1.12 ± 0.07 ($D_p \leq 10$ µm)	5561 ± 5476	726 ± 780	0.20 ± 0.24
GVAX	0.14 ± 0.12	1.23 ± 0.45	137.9 ± 120.6 ($D_p \leq 1$ µm) 218.9 ± 200.4 ($D_p \leq 10$ µm)	0.92 ± 0.03 ($D_p \leq 1$ µm) 0.93 ± 0.03 ($D_p \leq 10$ µm)	1.66 ± 0.27 ($D_p \leq 1$ µm) 1.45 ± 0.14 ($D_p \leq 10$ µm)	2597 ± 1797	1426 ± 1031	0.51 ± 0.29
FKB	0.12 ± 0.05	1.88 ± 0.27	48.3 ± 35.7 ($D_p \leq 1$ µm) 57.2 ± 44.3 ($D_p \leq 10$ µm)	0.84 ± 0.06 ($D_p \leq 1$ µm) 0.85 ± 0.06 ($D_p \leq 10$ µm)	1.33 ± 0.17 ($D_p \leq 1$ µm) 1.36 ± 0.17 ($D_p \leq 10$ µm)	3591 ± 2098	1007 ± 749	0.29 ± 0.17

* σ_{sp} at 450 nm [Mm^{-1}]; S = Supersaturation

ACPD
13, 23023–23056, 2013

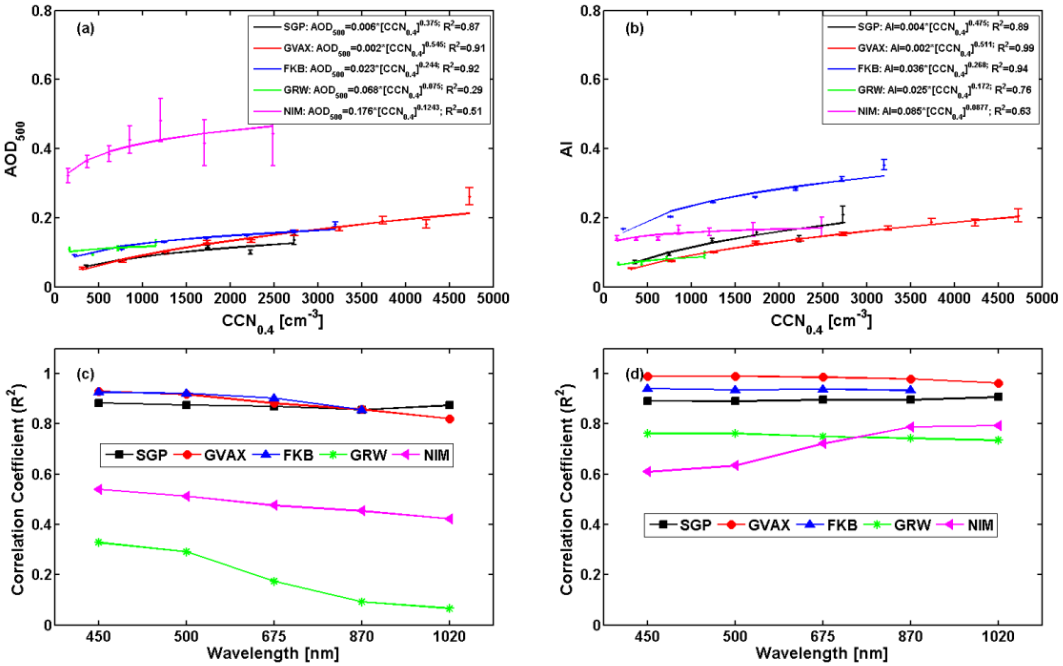

Fig. 1. (a) Relationship between AOD at 500 nm and $CCN_{0.4}$; **(b)** Relationship between AI and $CCN_{0.4}$. **(c)** Their correlation coefficients; and **(d)** same as **(c)** but for AI in lieu of AOD.

ACPD
13, 23023–23056, 2013

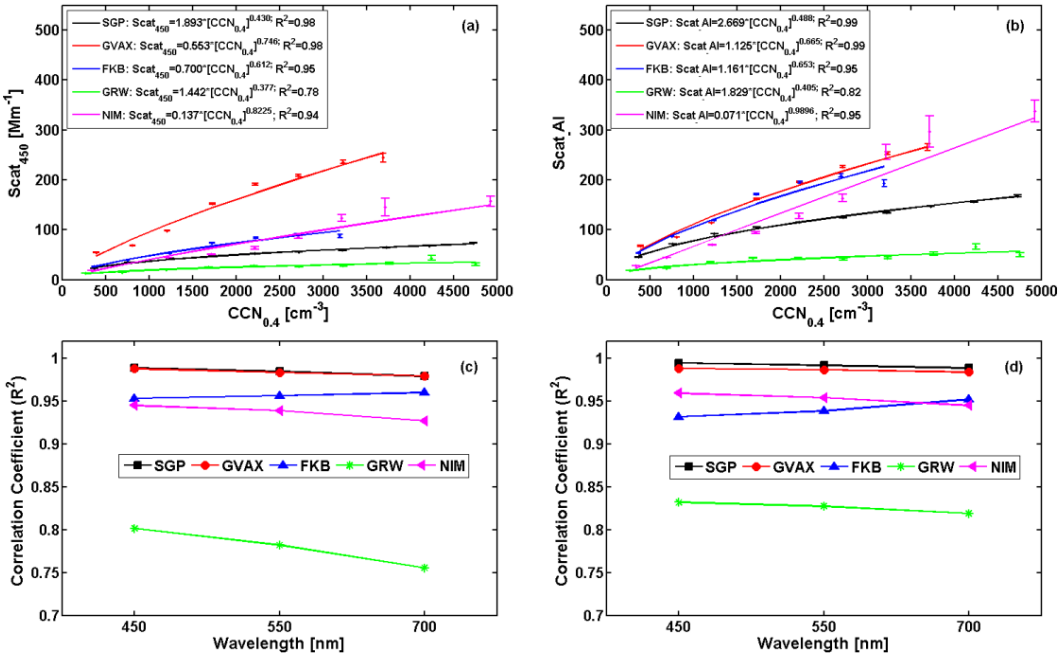

Fig. 2. Same as Fig. 1 but AOD is replaced by aerosol scattering coefficients for dry aerosol particles with diameters less than 1 μm measured by nephelometers.

ACPD
13, 23023–23056, 2013

Estimation of cloud condensation nuclei concentration

J. Liu and Z. Li

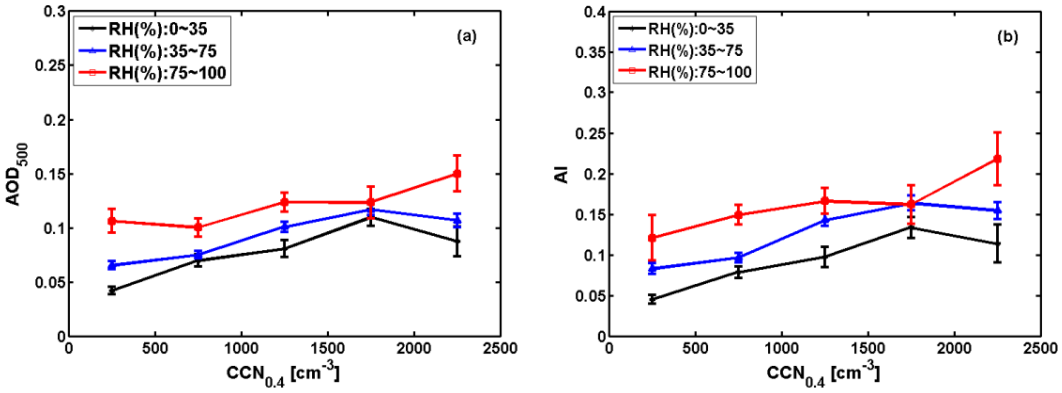

Fig. 3. Variations of $CCN_{0.4}$ concentration on **(a)** AOD at 500 nm and **(b)** AI for different ranges of ambient RH. Data are from the SGP site.

ACPD
13, 23023–23056, 2013

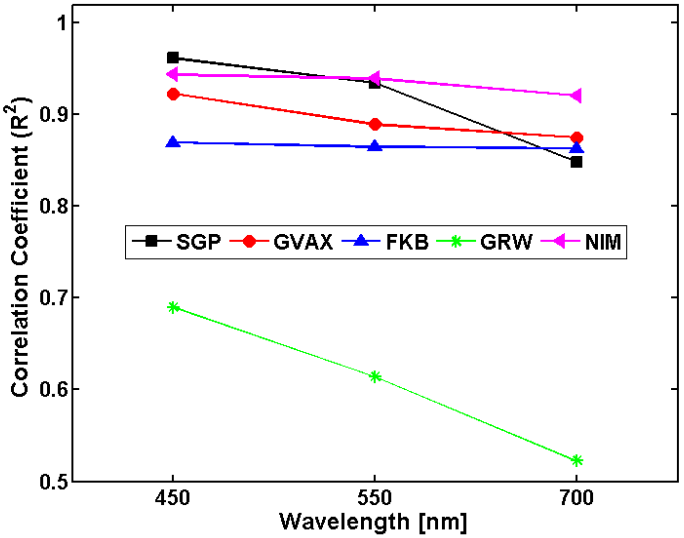

Fig. 4. Correlation coefficients of the relationship between surface-measured aerosol scattering coefficients and $CCN_{0.4}$ concentrations as a function of wavelength for ambient RH conditions and with diameters less than 1 µm.

ACPD
13, 23023–23056, 2013

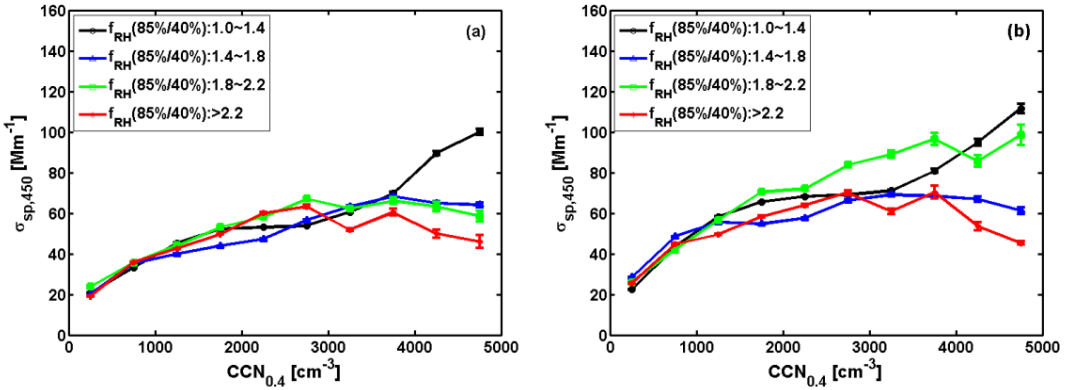

Fig. 5. Relationship between $CCN_{0.4}$ concentrations and aerosol scattering coefficients at 450 nm for dry aerosol particles with **(a)** $D_p \leq 1\,\mu m$ and **(b)** $D_p \leq 10\,\mu m$ for different ranges of aerosol hygroscopic growth factor. Data are from the SGP site.

ACPD
13, 23023–23056, 2013

Estimation of cloud condensation nuclei concentration

J. Liu and Z. Li

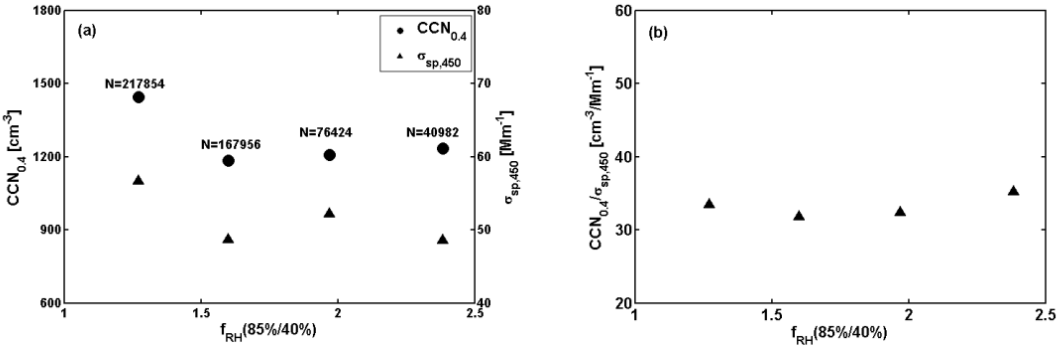

Fig. 6. (a) Dependence on f_{RH} of **(a)** $CCN_{0.4}$ and aerosol scattering coefficients and **(b)** their ratio for dry particles with $D_p \leq 1$ µm. Data are from the SGP site.

ACPD
13, 23023–23056, 2013

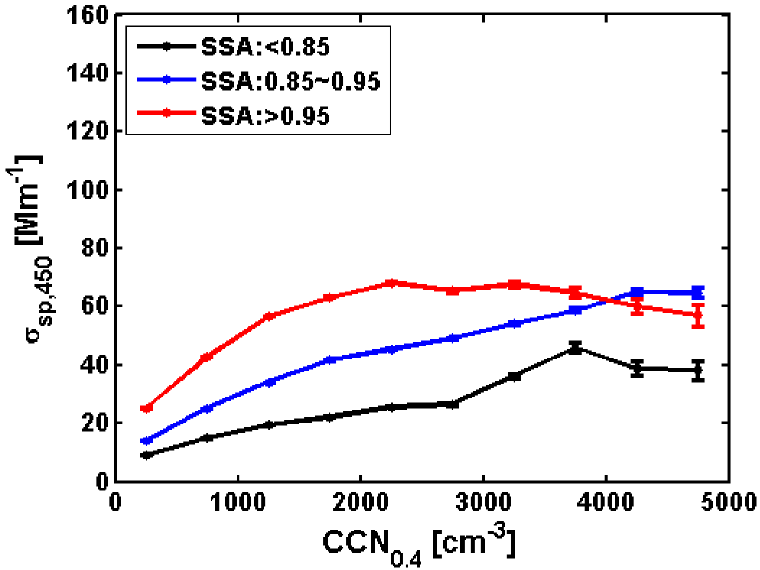

Fig. 7. Relationship between aerosol scattering coefficients at 450 nm and $CCN_{0.4}$ concentration for different ranges of SSA for dry particles with $D_p \leq 1$ µm.

ACPD
13, 23023–23056, 2013

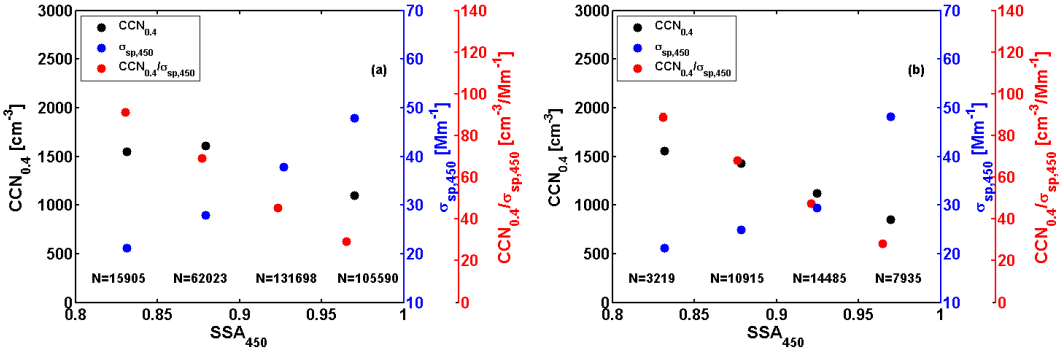

Fig. 8. $CCN_{0.4}$ concentration, aerosol scattering coefficient and their ratio as a function of SSA at 450 nm for all dry particles with $D_p \leq 1$ µm for **(a)** any value of the extinction Angstrom exponent and **(b)** between 1.6 and 1.8. The sample number in each SSA bin for each case is given in each panel.

ACPD
13, 23023–23056, 2013

Estimation of cloud condensation nuclei concentration

J. Liu and Z. Li